

# GRAPHENE BASED COMPOSITES FOR CORROSION INHIBITION OF STAINLESS STEEL 304

Hesham Alhumade<sup>1</sup>, Erij Elkamel<sup>2</sup>, Hiba Nauman<sup>3</sup>, Aiping Yu<sup>4</sup>, Ali Elkamel<sup>5</sup>

Department of Chemical Engineering

University of Waterloo

Waterloo, Ontario, Canada N2L 3G1

<sup>1</sup>[halhumade@uwaterloo.ca](mailto:halhumade@uwaterloo.ca)

<sup>2</sup>[aipingyu@uwaterloo.ca](mailto:aipingyu@uwaterloo.ca)

<sup>3</sup>[eelkamel@uwaterloo.ca](mailto:eelkamel@uwaterloo.ca)

<sup>4</sup>[hnauman@uwaterloo.ca](mailto:hnauman@uwaterloo.ca)

<sup>5</sup>[aekamel@uwaterloo.ca](mailto:aekamel@uwaterloo.ca)

**Abstract— Polyetherimide-Graphene (PEI/G) composites were prepared and investigated as anti-corrosion coatings on Stainless Steel 304 (SS304) substrates. A small load of graphene was incorporated in the polymeric matrix using in situ polymerization approach and the coating was cured under vacuum by several steps thermal imidization. The morphology was examined using Scanning Electron Microscopy (SEM) and Transmission Electron Microscopy (TEM). The study demonstrates that advanced corrosion inhibition of SS304 can be achieved by coating the metal with PEI and this inhibition can be further enhanced by incorporating graphene. This conclusion was supported by the collected results from electrochemical techniques such as Tafel polarization and electrochemical impedance spectroscopy (EIS). In addition to corrosion protection, the interface adhesion between the protected substrate and the protective coating was evaluated according to ASTM standards.**

**Index terms- Graphene, Adhesion, In situ polymerization, Thermal Imidization, Tafel polarization, Impedance Spectroscopy.**

## I. INTRODUCTION

An increasingly problematic issue in the metallic finishing industry is corrosion. Corrosion is the deterioration of materials due to electrochemical reactions that occur with their surroundings. Not only is corrosion a costly issue but it also affecting the economies of today's industrial nations. Therefore, a number of researchers worked on the design of advanced materials and coating alternatives that can significantly improve materials durability by protecting it from corrosion or at least slowing down the detrimental process. Studies have already shown the success of anti-corrosive coatings such as nanocomposites, hydrophobic and organic-inorganic hybrid coatings to extend the lifespan of materials [1]. Other techniques researched that also battle corrosion are

corrosion inhibitors [2], and anodic and cathodic protections [3,4]. Although the current protection technologies are being widely used in the construction, pipeline, and automobile industries, there is a demand for an even more efficient anti-corrosion technique that has a better inhibition efficiency, and that is cost effective.

SS304 has been widely used in the chemical process industry. SS304 is not only formable and weldable, but it also has substantial thermal and electrical conductivity. Additionally, SS304 can withstand a wide range of atmospheric conditions and temperatures up to 1650°F [5]. However, in sodium chloride solutions specifically, SS304 is shown to corrode more intensely [6].

Fillers in polymeric composites might have the dual application of both slowing the process of corrosion while also strengthening the mechanical properties of the material. The metal is protected from corrosion since the diffusion of harmful corrosive agents is limited by the anticorrosive layer in the coating which therefore sustains the metal substrate. The mechanical properties are strengthened as made clear by studies conducted on polymer based composites in the 1960's. This is especially true when nanofillers made with inorganic compounds formed organic-inorganic nanocomposites in layered, tubular, and spherical forms such as clay, carbon nanotubes and silicon dioxide. A challenge in manufacturing corrosion protective coatings is the lack of adhesion between polymeric substances and the metal substrates on which they are coated. Although these substances could have a significant contribution in corrosion protection, their lack of grip with the metal substrates becomes a barrier for them to be put to practical use [7]. Polyetherimide (PEI) however, is a polymeric material that is highly effective as it has high thermal and chemical stability, high temperature durability, a low dielectric constant, and a low thermal expansion coefficient [8]. Due to these desirable properties PEI is an ideal material to be used in the manufacturing of anticorrosion coatings.

A material that is being increasingly used in the manufacturing of polymers composites is graphene. Graphene improves

polymers mechanical, thermal and dielectric properties leading it to be a main topic in current and upcoming studies. These studies focus on using graphene in different materials such as graphene nanosheets, nanoplatelets and functionalized graphene as well [9]. Additionally, unlike other nanofillers graphene has a very low density and a very high aspect ratio [10]. It is due to these qualities that graphene based materials have found wide applications in corrosion protective coatings and also in gas barriers applications [11-15]. Both graphene and PEI evidently have properties of great significance. Regardless of this, little work has been done that combines both materials to form a composite to aid in the corrosion protection of stainless steel 304. This study focusses on the synthesis of a coating material using graphene-PEI (PEI/G) composites to shield the stainless steel 304 from air and water which are the main factors that cause corrosion. The coating provides further protection to the stainless steel as the well dispersed graphene nanosheets in the PEI matrix prolong the diffusion pathway for corrosion causing agents. The effectiveness of the graphene-PEI coating in this study is measured using electrochemical corrosion measurements in a 3.5 wt% aqueous sodium chloride solution. This test serves to measure the corrosion inhibition ability of the graphene-PEI nanocomposites.

- Materials and Methods

- Materials

SS304 foil supplied by Mc-Master-Carr was used for the experiments. Single layer graphene was used as provided by ACS Material, where it was prepared by thermal exfoliation/reduction of graphite oxide using the modified Hummer technique. According to the supplier, the single layer graphene has electrical resistivity of  $\leq 0.3 \Omega \cdot \text{cm}$  and surface area of 400-1000 m<sup>2</sup>/g. N-Methyl-2-pyrrolidone (NMP) solvent and m-Phenylenediamine (mPDA) were supplied by Sigma Aldrich. 4,4-Bisphenol A Dianhydride (BPADA) from Polysciences Inc. was stripped of moisture prior to use by vacuum at 60 °C for 3 h.

- Composite preparation, coating, and curing

Polyetherimide-Graphene composite coatings were prepared with graphene amounts of 0.1 wt. % (PEI/G<sub>0.1</sub>). The procedures are outlined below and represented in Figure 1.

In the preparation of PEI/G<sub>0.1</sub> coating, 6.4 mg of graphene was added to 35 mL of NMP and stirred for 1 h. Bath sonication was then carried out for an additional hour. 1.1 g of mPDA was added to 35 mL of NMP and stirred until the solution became clear. The graphene and mPDA solutions were combined and stirred for 1 h and then sonicated for 1 hour. Finally, 5.3 g of BPADA was added to the resulting solution and left to react overnight to ensure enough time for complete reaction. The final mixture was applied to a clean SS304 substrate using a brush and the thickness was maintained at  $50 \pm 1 \mu\text{m}$  through the use of a film applicator (Paul N. Gardner Company Inc.). The coated substrate was placed under vacuum for 10 h at 70 °C to evaporate the NMP solvent. The coating was then heated for 2 h each at 100 °C,

150 °C, and 205 °C. Finally, the coated substrate was left in the vacuum to cool to room temperature.

- Morphology Characterization

The graphene composite coating was analyzed using SEM (Zeiss LEO 1550) to observe the dispersion of the graphene fillers in the hosting polymeric matrix. The coated SS304 substrate was secured to the SEM holder with carbon tape and then gold coated by sputtering for 120 sec.

The morphology of the coating and the dispersion of graphene on the PEI matrix were also examined using TEM (Philips CM-10 TEM). A sample of the PEI/G coating was obtained by scraping it off the SS304 with a sharp knife. The sample was then soaked in methanol for 5 min, collected by a TEM copper grid, and left to dry overnight at room temperature under vacuum.

- Adhesion Test

The adhesion test was carried out as directed by the ASTM-3359D using a tape test kit (Paul N. Gardner Company Inc.) consisting of an 11-tooth blade with 1 mm spacing.

- Electrochemical Measurements

Electrochemical measurements were carried out with a VSP-300 workstation (Uniscan Instruments Ltd.) consisting of a double-jacketed corrosion cell with a three-electrode configuration. The cell was concealed by a Teflon plate with drilled holes for the electrodes to be placed through. The three-electrode cell comprised of a circular SS304 substrate serving as the working electrode (WE), two graphite rods as counter electrodes (CE) and silver/silver chloride (Ag/AgCl) as the reference electrode (RE). The SS304 specimen was cleaned with acetone and rinsed with distilled deionized water prior to use. It was then fixed in a Teflon sample holder with exposed area of 1cm<sup>2</sup> and the potential was allowed to stabilize in the 3.5 wt. % NaCl electrolyte solution at room temperature before conducting any test. All measurements were repeated three times to ensure data accuracy and reproducibility.

For determination of the corrosion potential ( $E_{\text{corr}}$ ) and corrosion current density ( $I_{\text{corr}}$ ), Bio-Logic EC-Lab software was used. The open circuit potential at equilibrium state was recorded as the open circuit potential (in mV) versus the reference electrode. Data was presented by Tafel plots within a range of -500 mV and +500 mV above the corrosion potential at a scan rate of 10 mV/min.  $I_{\text{corr}}$  was established by extrapolating the linear portions of the Tafel line to  $E_{\text{corr}}$ .

Electrochemical impedance measurements were carried out using the same software to obtain the Nyquist plots. The Bio-Logic EC-Lab was used to plot and fit the data at a frequency range of 100 kHz to 100 mHz. Corrosion rate ( $R_{\text{corr}}$ ) was calculated as per ASTM standard G102 using equation (1):

$$R_{corr} = \frac{0.13 \times I_{corr} \times EW}{A \times \rho} \quad (1)$$

Where EW is the equivalent weight of SS304 (25.12 g),  $\rho$  is the density of SS304 (8.03 g/cm<sup>3</sup>) and A is the sample area (1 cm<sup>2</sup>).

## I. Results and discussion

### o Morphology

The dispersion of graphene in the PEI matrix was captured using SEM and TEM at low and high magnifications as illustrated in Figure 2 and 3, respectively. Both figures represent a well dispersed graphene sheets in the PEI/G<sub>0.1</sub> coating. In particular, thin graphene sheets were captured in the PEI matrix in Figure 3, while stacks of graphene were observed in Figure 2.

### o Adhesion

The accumulation of corrosive agents in the void spaces at the interface between metals substrate and the protective coatings can be considered a major failure mechanism. Therefore, noble interface adhesion between metals and coatings is always a desire. In this study, the adhesion between SS304 and the PEI/G<sub>0.1</sub> coating was evaluated according to ASTM standard D3359 using the adhesion tape test kit. The adhesion tests results were captured using SEM and presented in Figure 4. From the figure, decent adhesion between the coating and the protected substrate was observed, where no peeling was witnessed and the PEI/G<sub>0.1</sub> received 5B rating (0% Peeling) according to ASTM D3359. This observation concluded that PEI/G<sub>0.1</sub> coating adhere well to the SS304 substrates and is a noble candidate for corrosion inhibition applications.

### o Potentiodynamic and Impedance measurements

Both Tafel polarization and Impedance spectroscopy are valuable techniques in corrosion mitigation evaluation. Therefore, both techniques were used to evaluate the degree of corrosion inhibition of PEI and PEI/G<sub>0.1</sub> coatings. Figure 5, depicts the Tafel plots for bare and coated SS304 substrates. In addition, Tafel plots were used to extract various corrosion parameters such as corrosion potential and corrosion current, which was obtained as the intersection between the extrapolation of the linear parts of both the anodic and the cathodic curves in the Tafel plots. The extracted parameters are reported in Table 1, where it can be observed that coating SS304 with PEI resulted in an increase in  $E_{corr}$  and a drop in  $I_{corr}$  and  $R_{corr}$ , which are signs of an enhancement in corrosion inhibition. Furthermore, the incorporation of graphene in the PEI matrix resulted in a further enhancement and attenuation of  $E_{corr}$  and  $I_{corr}$  and  $R_{corr}$ , respectively.  $I_{corr}$  magnitudes can be used to evaluate the protection efficiency ( $P_{EF}$ ) of the coatings using (2), where  $I_{corr}^{\circ}$  represents the corrosion current of bare SS304 substrate.

$$P_{EF} [\%] = [1 - I_{corr}/I_{corr}^{\circ}] \times 100 \quad (2)$$

EIS was also conducted to evaluate electrochemical activity on metals substrates. In impedance spectroscopy, a complex resistance known as impedance is observed when an alternative current passes through a circuit. In this study, impedance spectroscopy technique was used to examine the impedance behavior of the bare and coated electrodes. Furthermore, the impedance behavior of bare and coated SS304 was modelled using equivalent circuits, which are depicted in Figure 6, where  $R_s$ ,  $R_p$  and  $R_c$  represent the electrolyte, coating polarization and charge transfer resistances, respectively, CPE is a constant phase elements and W is the Warburg impedance.

The Nyquist plots for all samples are depicted in Figure 7. In general, an increase in the semi-circle size represents an enhancement in corrosion inhibition and consequently a slower corrosion rate. Furthermore, it was observed that the fitting data obtained from the equivalent circuits in Figure 6 fit well to the raw impedance data. The variation in the magnitudes of the various elements of the equivalent circuits can be used to evaluate the corrosion inhibition properties of the protective coatings. In particular, a higher charge transfer resistance reflects an enhancement in corrosion inhibition. The charge transfer resistances for bare, PEI and PEI/G<sub>0.1</sub> coated SS304 are 4009, 9508 and  $8.6 \times 10^5 \Omega \cdot \text{cm}^2$ , respectively.

Previously reported results in the Tafel polarization and impedance spectroscopy measurements concluded that PEI coating may enhance the corrosion mitigation on SS304 substrate. Furthermore, the incorporation of graphene can further corrosion protection even at a very low loading.

## II. Conclusion

Polyetherimide/graphene composite was prepared using thermal imidization and the dispersion of graphene was observed using SEM and TEM. The corrosion inhibition property of the prepared coating was evaluated using Tafel polarization and EIS. Furthermore, the interface adhesion between the SS304 substrate and the protective coating was evaluated according to an ASTM standard.

The results confirm that PEI coating can prolong the lifetime of SS304 substrate in corrosive medium such as 3.5 wt.% NaCl solution. Moreover, this protection property can be excelled by the incorporation of graphene even at a very low loading of 0.1 wt.%. The enhancement in the protection property after the incorporation of graphene can be a result of the ability of graphene in increasing the pathway corrosive agents follow to reach the coated substrate

## Acknowledgment

The authors would like to acknowledge the financial support by the Petroleum Institute, Abu Dhabi through research project # 66. The authors also acknowledge the financial

support and Mr. Alhumade full scholarship from the Ministry of Education, Kingdom of Saudi Arabia.

#### References

- Guo S F, Zhang H J, Liu Z, Chen W, Xie S F (2012) Corrosion resistances of amorphous and crystalline Zr-based alloys in simulated seawater, *Electrochem. Commun.* 24:39-42.
- Moretti G, Guidi F, Grion G (2004) Tryptamine as a green iron corrosion inhibitor in 0.5 M deaerated sulphuric acid. *Corros. Sci.* 46:387-403.
- [3] Shen G X, Chen Y C, Lin C J (2005) Corrosion protection of 316 L stainless steel by a TiO<sub>2</sub> nanoparticle coating prepared by sol-gel method. *Thin Solid Films* 489:130-136.
- Cecchetto L, Delabouglise D, Petit J P (2007) On the mechanism of the anodic protection of aluminium alloy AA5182 by emeraldine base coatings: Evidences of a galvanic coupling. *Electrochim. acta* 52:3485-3492.
- Kang G, Kan Q, Zhang J, Sun Y (2005) Time-dependent ratchetting experiments of SS304 stainless steel. *Int. journal of Plasticity* 22:858-894.
- The International Nickel Company Inc (1963) *Corrosion Resistance of the Austenitic chromium-nickel Stainless steels in chemical environments*, New York, pp. 1-19.
- Roy D, Simon G P, Forsyth M, Mardel J (2002) Towards a better understanding of the cathodic disbondment performance of polyethylene coatings on steel. *Adv. Polym. Technol.* 21:44-58.
- Crosby A J, Lee J (2007) Polymer nanocomposites: The nano effect on mechanical properties. *Polym. Rev.* 47:217-229.
- Potts J R, Shankar O, Du L, Ruoff R S (2012) Processing morphologyproperty relationships and composite theory analysis of reduced graphene oxide/natural rubber nanocomposites. *Macromolecules* 45:6045-6055.
- Xu Z, Buehler M J (2010) Geometry controls conformation of graphene sheets: Membranes, ribbons, and scrolls. *ACS Nano* 4:3869-3876.
- Chang C H, Huang T C, Peng C W, Yeh T C, Lu H I, Hung W I, Weng C J, Yang T I, Yeh J M (2012) Novel anticorrosion coatings prepared from polyaniline/graphene composites. *Carbon* 8:5044-5051.
- Chang K C, Hsu M H, Lu H I, Lai M C, Liu P J, Hsu C H, Ji W F, Chuang T L, Wei Y, Yeh J M, Liu W R (2014) Room-temperature cured hydrophobic epoxy/graphene composites as corrosion inhibitor for cold-rolled steel. *Carbon* 66:144-153.
- Singh B P, Jena B K, Bhattacharjee S, Besra L (2013) Development of oxidation and corrosion resistance hydrophobic graphene oxide-polymer composite coating on copper. *Surf. Coat. Tech.* 232:475-481.
- Chang K C, Hsu C H, Lu H I, Ji W F, Chang C H, Li W Y, Chuang T L, Yeh J M, Liu W R (2014) Advanced anticorrosive coatings prepared from electroactive Polyimide/graphene nanocomposites with synergistic effects

of redox catalytic capability and gas barrier properties. *Express. Polym. Lett.* 8:243-255.

- [15] Prasai D, Tuberquia J C, Harl R R, Jennings G K, Bolotin K I (2012) Graphene: corrosion-inhibiting coating. *ACS Nano* 6:1102-1108

**Figure Captions:**

**Fig. 1:** A graphical description of the synthesis of PEI/G composites using in situ polymerization procedure.

**Fig. 2:** SEM images for the dispersion of graphene at low and high magnifications in PEI/G<sub>0.1</sub> composite.

**Fig. 3:** TEM images for the dispersion of graphene at low and high magnifications in PEI/G<sub>0.1</sub> composite.

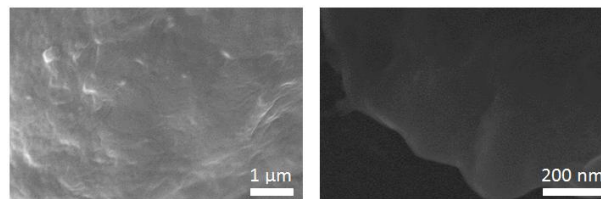
**Fig. 4:** SEM images for post-adhesion test on PEI/G<sub>0.1</sub> coating.

**Fig. 5:** Tafel plots for Bare SS304, PEI and PEI/G<sub>0.1</sub> coated SS304 substrates.

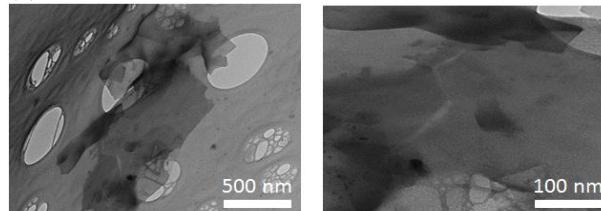
**Fig. 6:** Equivalent circuit for modeling the impedance behavior of (a) Bare SS304, (b) PEI and PEI/G<sub>0.1</sub> coated SS304 substrates.

**Fig. 7:** Nyquist plots for Bare SS304, PEI and PEI/G<sub>0.1</sub> coated SS304 substrates.

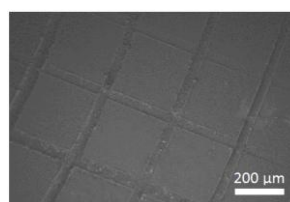
(1)



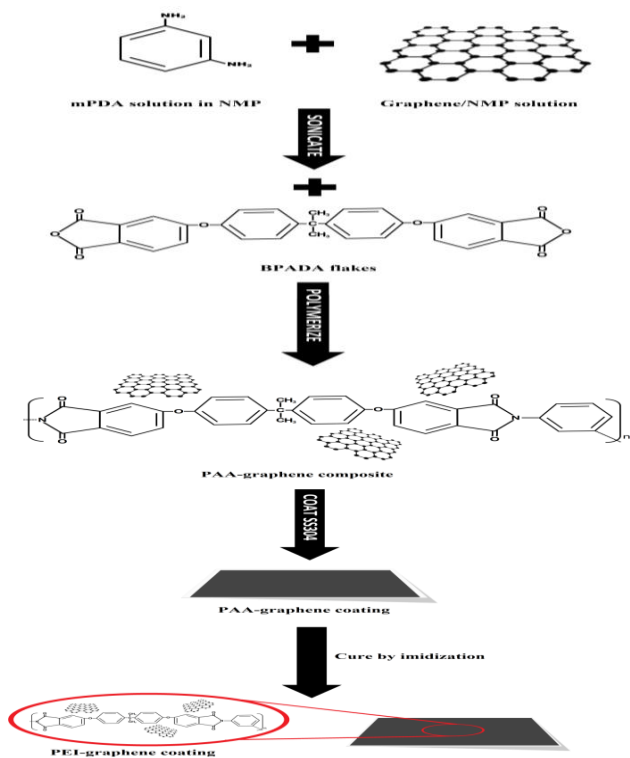
(2)



(3)



(4)



(5)

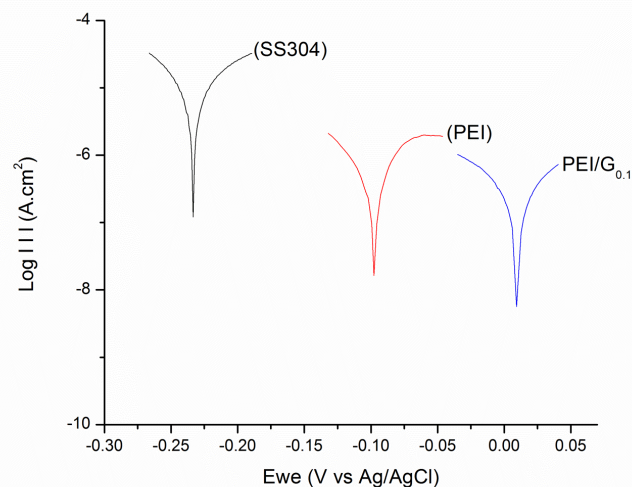
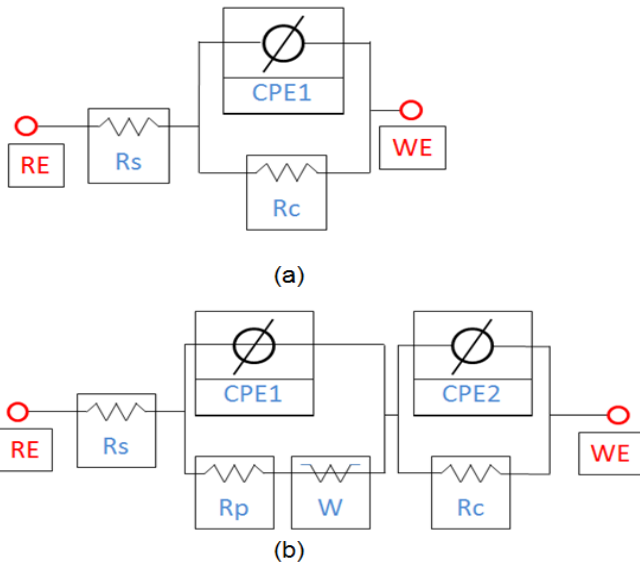
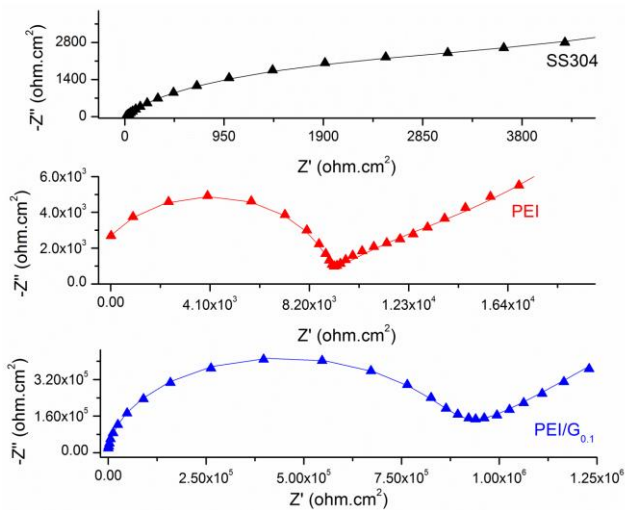


**Table I:** Corrosion parameters extracted from potentiodynamic measurements for Bare SS304, PEI and PEI/G<sub>0.1</sub> coated SS304 substrates in 3.5 wt.% NaCl Solution.

Sample	Corrosion Parameters Extracted From Tafel Plots			
	$E_{corr}$ [mV vs Ag/AgCl]	$I_{corr}$ [ $\mu\text{A}/\text{cm}^2$ ]	$R_{corr}$ [MPY]	$P_{EF}$ [%]
SS304	-239.2	1.2	0.48	-
PEI	-100.4	0.039	0.016	96.7
PEI/G <sub>0.1</sub>	17.9	0.029	0.012	98



(6)



(7)